Optical Properties of Si−Ge Semiconductor Nano-Onions

Nicola A. Hill*

Materials Department, University of California, Santa Barbara, California 93106

Simone Pokrant

Institut für Physikalische Chemie der Universität Bonn, Wegelerstr. 12, 53115 Bonn, Germany

Adrian J. Hill

Bell Laboratories, Lucent Technologies, 600 Mountain Ave., Murray Hill, New Jersey 07974

Received: January 14, 1999

We explore theoretically the possibility of obtaining efficient light emission from Si−Ge semiconductor nano-onions. Our motivation stems from the strong luminescence recently observed from II−VI nano-onions, combined with the technological significance of the Si−Ge system. We calculate the electronic properties of a range of hypothetical Si−Ge nano-onions using the tight-binding method and determine the combination of size, strain, and materials which optimizes the production of visible luminescence. We predict that small (less than around 30 Å diameter) Si-covered Ge nano-onions will be visible light emitters.

1. Introduction

Semiconductor nanocrystals are nanometer-sized crystallites of semiconducting material, with similar lattice structure and lattice constant to the corresponding bulk semiconductor. Nanocrystals are of fundamental physical interest because their electronic and optical properties are markedly different from those of bulk semiconductors and depend strongly on the size of the structure. Small crystallites have photophysical properties similar to those of large molecules, in which the electrons occupy discrete molecular orbitals. Large crystallites show bulk-like semiconductor properties, with the electrons and holes occupying continuous bands in the crystal. In the intermediate size region, the band gap, and corresponding optical and electronic properties, are sensitive to the number of atoms in the nanocrystal.

The size dependence of the electronic properties leads to a number of potential device applications. In this paper we focus specifically on the size dependence of the exciton energy, and the corresponding application of visible luminescence from Si−Ge systems. The exciton energy is determined by the electron−hole Coulomb attraction and by the size of the band gap. Therefore, both the energy required to form an exciton and the energy released when the exciton recombines depend on the size of the nanocrystal. This leads to potential applications of nanocrystals in wavelength tunable light emission or detection. One application which is being actively pursued is the use of nanocrystals as the luminescent component in light emitting diodes (LEDs). Here, the wavelength of the emitted light is determined by the size of the nanocrystal.[2]

Nanocrystals are typically grown using colloidal chemical synthesis[1] which produces highly monodisperse samples over a broad size range (between around 10 and 1000 Å diameter). Such colloidal nanocrystals offer many advantages over more traditional nanometer-sized quantum dot structures fabricated using molecular beam epitaxy (MBE). They can be produced cheaply and in macroscopic quantities, with narrow size distributions over a range of diameters.[1] The surfaces are terminated with organic ligands which stabilize the nanocrystals and provide solubility. This allows for easy manipulation; for example, the individual nanocrystals can be assembled into three-dimensional crystals[3] or small molecules, in which each "atom" is a quantum dot.[4] In addition they can be incorporated into polymers or thin films of bulk semiconductors.[5] Also, free-standing nanocrystals are more able to relax strain than embedded, MBE-grown dots. However one significant disadvantage of colloidal nanocrystals terminated by organic ligands is that the luminescence is rather inefficient.[6] This is a result of gap surface states resulting from surface reconstructions, surface nonstoichiometry, and the incomplete saturation of surface dangling orbitals. In the next section we discuss one approach which has recently been developed to overcome this deficiency.

2. Semiconductor Nano-Onions

The terms "semiconductor nano-onion" or "core−shell particle" refer to nanocrystals which consist of a core of one semiconducting material, surrounded by a shell (or shells) of different, epitaxially matched, semiconductors. The resulting concentric shells of different semiconducting materials resemble the layers of an onion. A number of material combinations have been synthesized, including CdS-coated CdSe,[7] ZnS-coated CdSe,[6] and alternating CdS−HgS layers.[9] In all cases, the epitaxial matching provides superior surface termination of the core material, compared with capping the surface with organic ligands. The epitaxy and passivation in nano-onions is now comparable to that of MBE-grown quantum dots.[10] In addition, because the synthesis is still achieved by chemical methods, and the outer surface of the *shell* is still terminated by organic ligand molecules, all the advantages of colloidal nanocrystals over MBE-grown nanostructures are retained.

The electronic and optical properties of semiconductor nano-onions depend on the band structures of both constituent

* Corresponding author. E-mail: nahill@mrl.ucsb.edu.

10.1021/jp990188c CCC: $18.00
Published on Web 04/02/1999

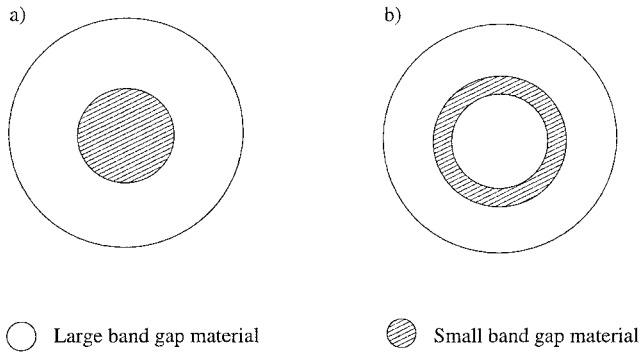

Figure 1. Figure 1. Schematic cross sections of semiconductor nano-onions: (a) a small band gap core surrounded by a large band gap shell; (b) a large band gap core, a small band gap "sandwich" layer, and a large band gap outer layer.

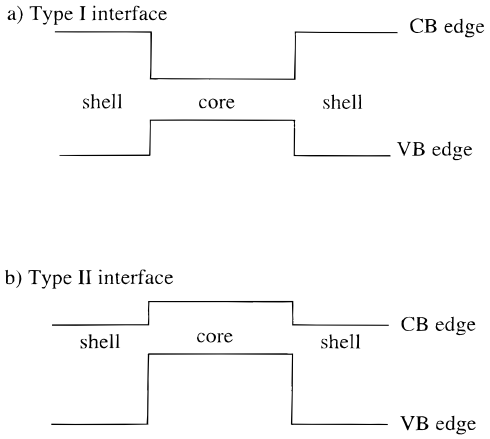

Figure 2. Schematic band diagram of semiconductor nano-onions. A region of small band gap materials is surrounded on both sides by a region of large band gap material: (a) a nano-onion with a type I interface, in this case the small band gap material has a higher valence band edge and a lower conduction band edge than the large band gap material; (b) a nano-onion with a type II interface. Here, the band edges of the small band gap material are either both higher or both lower in energy than the corresponding band edges in the large band gap material.

materials. Two scenarios are of interest. The first is a core of small band gap material, surrounded by a shell of large band gap material, as shown schematically in Figure 1a. An example is a CdSe cluster coated with CdS. Such clusters have been grown and have been shown to be photostable and highly luminescent.[7] LEDs made with these nano-onions show enhanced luminescence compared with the regular II−VI nanocrystals.[11]

The second is a layer of small band gap material sandwiched between a large band gap core and a large band gap shell, as sketched in Figure 1b. These were the first type of semiconductor nano-onions to be synthesized, using CdS as the large band gap material and HgS for the sandwich layer.[9]

In both cases, the small band gap material forms a quantum dot with the surface essentially perfectly passivated by the epitaxially grown large band gap material. When an electron hole pair is created in the nano-onion, both the electron and hole should be confined to the small band gap region so that they can recombine efficiently. Therefore the type I interface band diagram, shown schematically in Figure 2a, is desirable. The absorption and luminescence spectra are dominated by the small band gap material, but the intensity of the luminescence is dramatically enhanced over that in "regular" semiconductor nanocrystals. For example, Hines and Guyot-Sionnest[6] synthesized nano-onions of CdSe coated with a shell of ZnS (a type I interface) and compared the resultant luminescence intensity with that of CdSe nanocrystals terminated with tri-*n*-octylphosphine oxide (TOPO) organic ligands. They found that the luminescence intensity from the ZnS-coated particles was approximately 6 times greater than that from the particles terminated by organic ligands. Less desirable is the type II interface, shown in Figure 2b. In the example shown, the hole wave function would be concentrated in the core of the nano-onion, but the electron would localize on the surface states. Earlier theoretical work on CdS-coated CdSe particles[8] showed predominantly type II character, but with some spatial overlap of electrons and holes in both core and shell regions.

3. Si−Ge System

Silicon-based microelectronics is a multibillion dollar industry with a huge financial incentive to retain compatibility with Si processing in new devices. With traditional silicon technology nearing its limits for many applications, the Si−Ge system offers a new avenue for development without forcing a costly transition to a new material.[12] Attempts to use Ge to modify the properties of Si include growth of Si−Ge superlattices and formation of Si−Ge alloys.[13] Desirable properties of the new modified Si-based materials include higher electron mobilities and increased luminescence efficiency.[14] In addition, the Si and Ge lattices have a 4% mismatch, which might allow integration of different semiconductor materials (with their associated device functions) on Si substrates or novel devices requiring strain engineering.

In this work, we explore theoretically the possibility of obtaining efficient light emission from Si−Ge nano-onions. All nano-onions synthesized to date have been composed of II−VI materials. Although attempts to synthesize Si−Ge nano-onions have not yet begun, nanocrystals of Si and Ge have been grown with reasonable size selectivity and crystallinity. The synthetic techniques developed for the production of ionic II−VI nanocrystalline colloids are not readily applicable to the homoatomic group IV semiconductors, but a number of alternative synthetic methods have been explored. Colloidal nanocrystals of Ge have been grown in different size distributions using an inorganic solution phase synthesis.[15] In addition, Ge nanocrystals have been formed by implantation of Ge ions in a silicon dioxide matrix.[16] Also, arrays of Ge quantum dots have been grown by selective etching of SiO_2 and subsequent deposition of Ge in the remaining nucleation sites.[17] Si nanocrystals have been synthesized using spark ablation from a crystalline Si substrate,[18] high-temperature aerosol reaction,[19] and ion implantation into a silicon dioxide matrix.[6] In all cases, luminescence is observed at a wavelength which is shorter than the bulk band gap. This is believed to be the result of quantum confinement, although alternative explanations, such as recombination on surface species, have not been discounted.

The bulk band gaps of Si and Ge are around 1.1 and 0.75 eV, respectively. Therefore, we might expect to obtain the most efficient luminescence by surrounding Ge (the small band gap material) with Si (the large band gap material). However, the offset between the valence band edge energies in Si and Ge (calculated using density functional theory within the local density approximation[39] is more than 0.5 eV. This should cause the Si−Ge interface to be type II, giving poor luminescence from the nano-onions. Two factors act to override this simplified assumption.

First, the quantum confinement effect causes the band gaps of both Si and Ge to increase as the size of the nanocrystal is reduced. Because the confinement effect is stronger in Ge than in Si, there is a certain critical radius below which the band

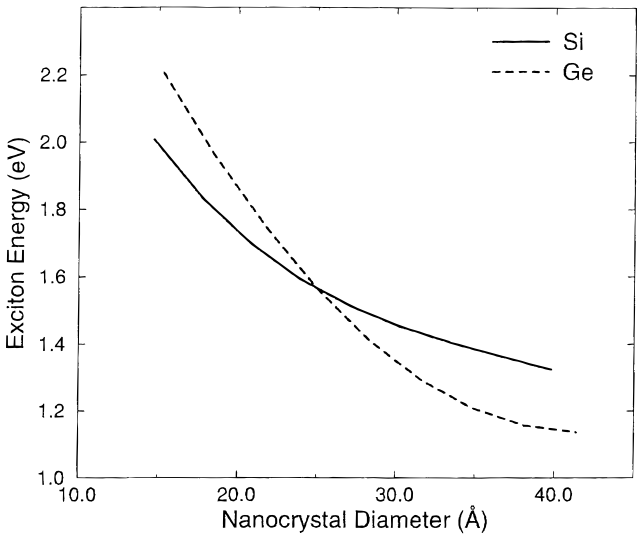

Figure 3. Exciton energies of Si and Ge nanocrystals as a function of diameter, calculated with the tight-binding parameters used in this work. The exciton energies were calculated for a range of nanocrystal sizes, and the lines show fits to those discrete values.

gap of the Ge nanocrystal is larger than that of the Si nanocrystal. This was first predicted by Takagahara and Takeda[20] who showed that, within the effective mass approximation, the exciton energy (that is, the band gap, corrected for the Coulomb interaction between the electron and hole) of Ge is larger than that of Si, below around 60 Å diameter. This faster increase of Ge band gap as the quantum dot size is reduced can be explained by its smaller effective mass. Figure 3 shows exciton energies for Si and Ge nanocrystals calculated in this work and in ref 21 using the tight-binding method described in section 4. The nanocrystals were constructed by building concentric shells of atoms around a central atom, and the band gaps were calculated for a range of cluster sizes. The plotted lines are polynomial fits to the calculated band gap energies. For comparison with Takagahara and Takeda's results, the band gap was corrected for the Coulomb interaction using the effective mass formula proposed by Brus,[22] with the bulk dielectric constant used for screening.[23] Using the tight-binding method, we obtain a critical diameter of around 25 Å below which the Ge exciton energies are larger than those of Si.

Second, strain in the lattice alters the band gap. The lattice constants of Si and Ge are 5.43 and 5.65 Å, respectively, a 4% lattice mismatch. Therefore, if epitaxial lattice matching is achieved at the Si−Ge interface, one or both of the materials must be strained. Qualitatively, if the Si is "stretched" to match the Ge, then there is less overlap between the Si atoms, giving narrower Si bands and a wider band gap. Conversely, if the Ge is compressed to match the Si lattice, then Ge orbitals on adjacent atoms interact more strongly, giving wider bands and a narrower gap.

In the remainder of this paper, we present the calculated electronic structures of a range of Si−Ge nano-onions, with various combinations of strained and relaxed Si and Ge cores and shells, including relaxed atomic configurations with minimized strain energy. The most likely candidates for obtaining visible luminescence are discussed in the concluding section.

4. Theoretical Technique

We calculate the electronic properties of the nano-onions using a tight-binding Hamiltonian, with an sp^3s^* basis set which includes only nearest-neighbor interactions.[3] Within this simple basis, the tight-binding matrix can be diagonalized directly, using Jacobi transformation, to obtain the nanocrystal's eigenvalues and eigenfunctions. This Hamiltonian was used in earlier work on Si nanocrystals,[21] and although it is less rigorous than techniques adopted by other workers (see for example refs 31−33), the calculated band gaps are within the uncertainty range of the most recent experimental data.[34]

Lattice strain is included in the calculation using the parametrization proposed by Brey et al.,[35]

$$h = h_0\left(\frac{d}{d_0}\right)^{-\alpha} \tag{1}$$

where h_0 is the tight-binding matrix element at the equilibrium bond length, d_0, and h is the matrix element at the new bond length, d. The parameter α is computed in ref 35 using self-consistent Wannier functions. For Si, α is close to the value of 2 proposed by Harrison[36] for all the off-diagonal Hamiltonian matrix elements. However, contrary to Harrison's proposal, the diagonal, intraatomic parameters also scale with bond length, because the energy difference between the s and p levels changes. In Ge, the value of α deviates markedly from 2 and is strongly orbital dependent. The adequacy of this model for describing strained Si−Ge has been tested by comparing the experimental deformation potentials with those calculated within the model. Reference 37 computes the hydrostatic direct ($a^c - a^v$) and indirect ($E_1 + a^v)^\delta$ and uniaxial (b and Ξ_u^v) deformation potentials. All results, except for Ξ_u^v are within 10% of the experimental values, and the larger deviation in Ξ_u^v leads to an error of only a few hundredths of an electronvolt in the bottom of the conduction band.

Two problems arise in the use of bulk tight-binding parameters to describe semiconductor heterojunctions. First, the energy zeros in both materials must be chosen so as to obtain the correct shift in the band edges across the interface. This problem has been discussed extensively (see for example ref 38 and references therein), and a number of solutions have been proposed. These include fitting to differences in measured photothresholds or electron affinities of the bulk materials, matching the energies of the dangling sp^3 hybrid orbitals (the "neutrality level") on either side of the interface, or using universal parameters and atomic term values for all parameters. In this work, we use the results of a first-principles calculation for a Si−Ge superlattice performed using a plane wave pseudopotential implementation of density functional theory within the local density approximation.[39] The first-principles results give a value of 0.54 eV for the valence band offset. Second, tight-binding parameters must be chosen for the interface layer, which in this case consists of Si−Ge bonds. We use the average values of the Si−Si and Ge−Ge tight-binding parameters,[40] although there is no rigorous physical justification for this choice.

Earlier studies showed that the choice of termination for the surface of the nanocrystal can have a large effect on the density of states in the band gap region.[25] In this work, we are interested in nano-onions where the electron and hole are confined to the core region of the cluster and have minimal spatial overlap with the outer surface of the shell. Therefore, rather than including a detailed model of the outer surface, instead we artificially remove all surface dangling orbitals from the Hamiltonian matrix before diagonalization.

The atomic positions which minimize the strain energy are calculated using a conjugate gradient implementation of Keating's valence force field method.[26] A detailed description of

TABLE 1: Band Gaps and Spatial Distribution of the Valence (VB) and Conduction (CB) Band Edge Eigenstates between Core and Shell Regions[a]

			VB edge		CB edge	
core	shell	band gap (eV)	core %	shell %	core %	shell %
relaxed Ge	strained Si	1.52	74	26	80	20
relaxed Si	strained Ge	1.62	50	50	22	78
strained Ge	relaxed Si	1.40	74	26	88	12
strained Si	relaxed Ge	1.71	48	52	22	78

[a] The data are for 30 Å diameter nano-onions with 20 Å diameter cores (calculated in this work using the tight-binding method).

this atomistic approach to calculating inhomogeneous strain between lattice mismatched interfaces is given in ref 27. For this work, we use the valence force field parameters of ref 28, which were obtained by fitting to the results of ab initio total energy calculations for Si, Ge, and Si−Ge.

5. Calculated Properties of Si−Ge Nano-Onions

We begin by calculating the electronic properties of approximately spherical nanocrystals containing a total of 525 atoms, of which 147 are in the core, and the remainder are in the shell. This corresponds to a core diameter of around 20 Å, and a total diameter of 30 Å. There are four end-point scenarios. The first is a nanocrystal with a relaxed Ge core and a Si outer shell strained epitaxially to match it. This would correspond to the case of growth of a Ge particle, then addition of Si to the outer surface. The second is the corresponding relaxed Si core surrounded by a strained Ge shell. We initially model the shell layers with a constant, homogeneous strain. This is a reasonable approximation for the layers in the immediate vicinity of the interface, although in a true free-standing cluster, the strain would undoubtedly relax in the outer surface region. In section 6, we present results for such relaxed, strain-minimized nano-onions. The third is a cluster consisting of a shell of Si at its equilibrium lattice constant, containing Ge within it, strained to match the Si. This scenario might be achieved by growth of Ge nanocrystals within a Si wafer after ion implantation. The final scenario is a strained Si core within a relaxed Ge shell. Again "real" nanocrystals will distribute the strain between both the Si and Ge layers and will represent a case intermediate between these extremes, as discussed in the next section.

Table 1 summarizes the calculated band gaps for these four limiting cases. We do not convert the band gaps to exciton energies by including the electron−hole Coulomb interaction at this stage, since calculation of the dielectric screening in a quantum dot containing two materials is beyond the scope of this work. All four nano-onions have band gaps close to the red end of the visible spectrum; therefore, based on consideration of the band gaps alone, all four core/shell arrangements could be candidates for visible light emission. However, an equally important factor is the extent of confinement of the electron and hole wave functions to the core regions. The percentage of the band edge eigenstates in the core and shell regions is also listed in Table 1. Regardless of whether the Si is strained or relaxed, when it forms the core of the nano-onion, the state at the top of the valence band contains approximately 50% core and 50% shell contributions. More than 75% of the state at the bottom of the conduction band is located in the shell region, with only a small amount of core contribution. Therefore, if an exciton is created in this nano-onion, the electron and hole are likely to trap on surface states and combine nonradiatively. This is exactly the opposite of the effect that we are looking for.

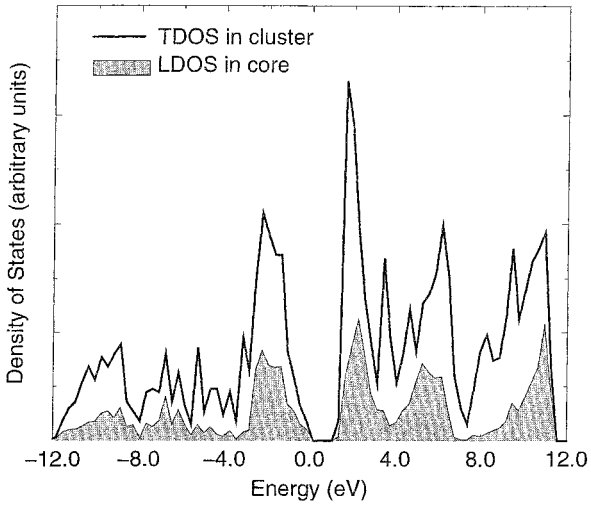

Figure 4. Density of states in a 30 Å diameter Ge-covered Si nano-onion. The Si is strained to match the Ge lattice constant. The solid line shows the total density of states (TDOS) in the particle, and the shaded region is the local density of states (LDOS) in the Si core region.

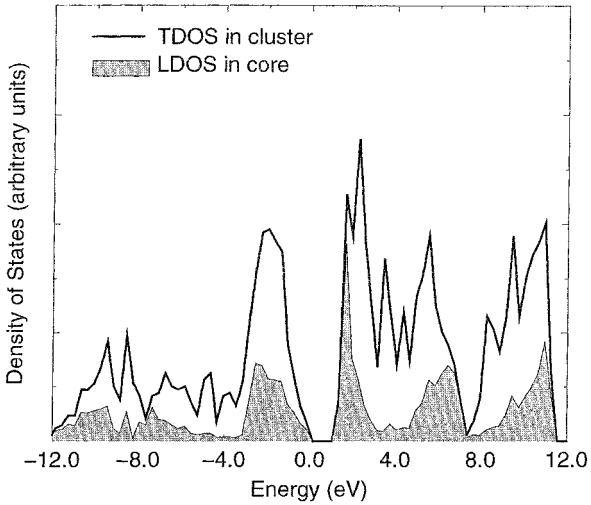

Figure 5. Density of states in a 30 Å diameter Si-covered Ge nano-onion. The Si is strained to match the Ge lattice constant. The solid line shows the total density of states (TDOS) in the particle, and the shaded region is the local density of states (LDOS) in the Si core region.

Figure 4 shows the calculated density of states in the particle with a strained Si core surrounded by a relaxed Ge shell. The solid line shows the total density of states (TDOS) in the particle, and the shaded region is the local density of states (LDOS) in the Si core region. The zero of energy is set to the top of the valence band in bulk Si. The valence and conduction bands are clearly visible, and the band gap is increased over the bulk Si and Ge values. It is apparent from the LDOS plot that the states around the band edges contain a significant amount of shell contribution.

However, when the core of the nano-onion is made of Ge, analysis of the band edge eigenstates shows that 75% of the valence band edge state is confined to the core region, and the conduction band edge state is at least 80% in the core. Since both the highest valence band state and the lowest conduction band state are located in the core region, this arrangement forms a quantum dot with a type I interface. So we expect such nano-onions to have strong luminescence. As an example, Figure 5 shows the calculated density of states in the nanocrystal consisting of a Ge core surrounded by a Si shell strained to

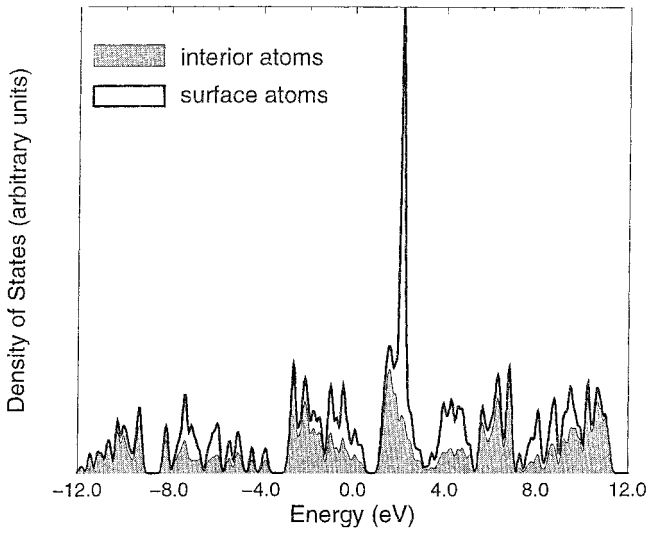

Figure 6. Density of states in a 20 Å diameter Ge nanocrystal without surface passivation. The solid line is the total density of states, the gray scale is the contribution from the interior atoms, and the unshaded area is the contribution from the surface atoms.

match the Ge lattice constant. Again, the solid line shows the total density of states, with the local density of states in the core region shaded gray. In this case, the band edges are composed predominantly of core states.

For contrast, Figure 6 shows the calculated density of states in a nanocluster of pure Ge of the same size as the Ge core in the previous example. In this case, the surface dangling bonds are unpassivated.[41] The surface dangling orbitals contribute many states around the band gap region, which will quench the luminescence.

6. Strain-Minimized Nano-Onions

In this section, we investigate the effects of allowing the atoms to relax to the positions which minimize the total strain energy in the nano-onion. Parts a and b of Figure 7 show the resulting calculated bond lengths in strain-minimized 525-atom nano-onions with 147-atom Si and Ge cores, respectively. The solid lines show the average bond lengths in each shell around the central atom (shell 0), and the dashed lines indicate the bond lengths in the bulk materials. In both cases, the bond lengths in the core relax almost uniformly in the direction of the average bond length. The bond lengths in the shell vary from approximately the average bond length at the interface to almost the bulk value at the surface.

The calculated band gaps for the strain-minimized nano-onions are intermediate between those of the corresponding nano-onions with strained and relaxed cores. The nano-onion with the Si core has a band gap of 1.64 eV, and around $^2/_3$ of both band edge eigenstates confined to the shell region. The nano-onion with the Ge core has a band gap of 1.45 eV and around 80% of both band edge eigenstates localized in the core. Therefore, our earlier suggestion that Si-coated Ge nano-onions are suitable candidates for visible photoluminescence is confirmed by these calculations for nano-onions with realistic strain profiles.

7. Conclusions

We have shown that epitaxial matching of Si around a core of Ge will produce a nano-onion in which the Ge forms a quantum well. The quantum well will confine the electron hole pair and promote efficient luminescence. The band gap will be

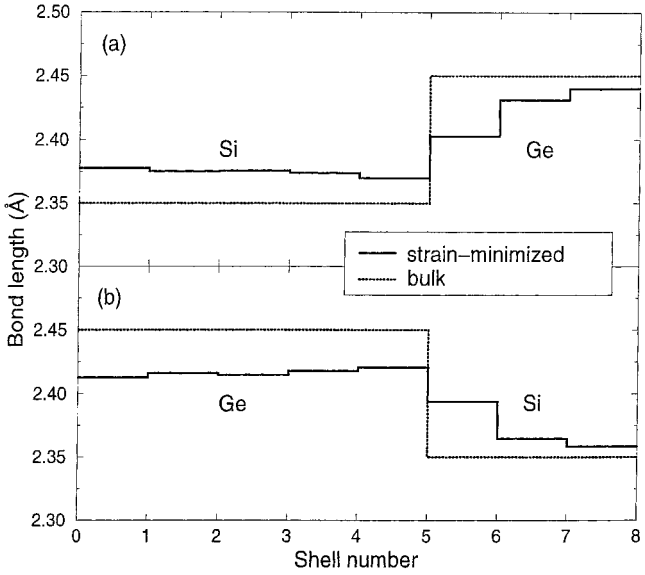

Figure 7. Calculated bond lengths in 525-atom strain-minimized Si−Ge nano-onions. The solid lines show the average bond lengths in each shell around the central atom (shell 0), and the dashed lines indicate the bond lengths in the bulk materials. The nano-onions in (a) consist of a 147-atom Si core surrounded by three atomic layers of Ge; (b) consists of a 147-atom Ge core surrounded by three atomic layers of Si.

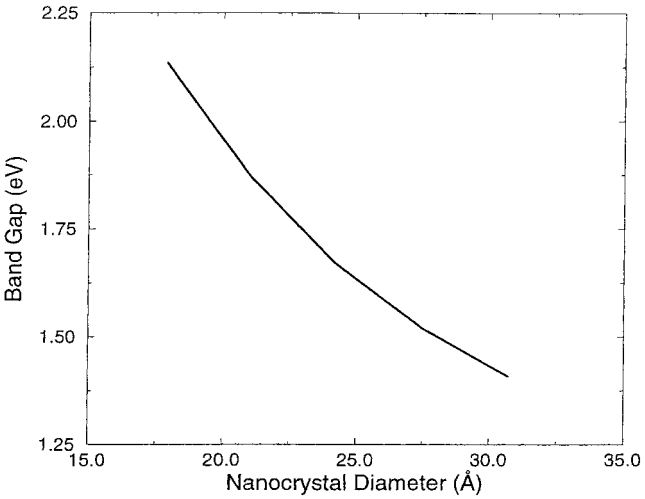

Figure 8. Variation in band gap with crystallite size for nano-onions consisting of a relaxed Ge core surrounded by a strained Si shell. The band gaps were calculated for a range of nano-onion diameters, and the line is a fit to the discrete values. For all onions, the width of the Si shell is 5 Å (three layers of atoms).

largest if the Ge lattice constant is maintained and the Si is strained to match it. Finally, in Figure 8, we show the calculated variation in band gap as a function of nanocrystal size for nano-onions consisting of a relaxed Ge core surrounded by an epitaxially matched Si shell. The width of the Si shell is 5 Å in all cases. Below around 30 Å diameter, the band gap is within the visible region of the spectrum. Therefore, we conclude that achieving the synthesis of small Si-coated Ge nano-onions might open an alternative route for obtaining light emission from Si-based structures. It will be interesting to see if this prediction can be confirmed by experiment soon.

References and Notes

(1) Murray, C. B.; Norris, D. J.; Bawendi, M. G. *J. Am. Chem. Soc.* **1993**, *115*, 8706.

(2) Colvin, V. L.; Schlamp, M. C.; Alivisatos, A. P. *Nature* **1994**, *370*, 354.
(3) Murray, C. B.; Kagan, C. R.; Bawendi, M. G. *Science* **1995**, *270*, 1335.
(4) Alivisatos, A. P. *Science* **1996**, *271*, 933.
(5) Kagan, C. R.; Murray, C. B.; Nirmal, M.; Bawendi, M. G. *Phys. Rev. Lett.* **1996**, *76*, 1517.
(6) Hines, M. A.; Guyot-Sionnest, P. *J. Phys. Chem*. **1996**, *100*, 468.
(7) Peng, X.; Schlamp, M. C.; Kadavanich, A. V.; Alivisatos, A. P. *J. Am. Chem. Soc.* **1997**, *119*, 7019.
(8) Pokrant, S.; Whaley, K. B. *J. Chem. Phys*., submitted.
(9) Mews, A., et al. *J. Phys. Chem*. **1994**, *98*, 934. Schoss, D.; Mews, A.; Eychmüller, A.; Weller, H. *Phys. Rev. B* **1994**, *49*, 17072.
(10) Gossard, A. C. *IEEE J. Quantum Elec.* **1986**, *22*, 1649.
(11) Schlamp, M. C.; Peng, X.; Alivisatos, A. P. *J. Appl. Phys.* **1997**, *82*, 5837.
(12) Cressler, J. D. *IEEE Spectrum* **1995**, 49.
(13) Meyerson, B. S. *Phys. Today* **1994**, 62.
(14) König, U. *Microelectron. Eng.* **1994**, *23*, 3.
(15) Heath, J. R.; Williams, R. S.; Shiang, J. J.; Wind, S. J.; Chu, J.; D'Emic, C.; Stanis, C. L.; Bucchignano, J. J. *J. Phys. Chem.* **1996**, *100*, 3144.
(16) Atwater, H. A.; Shcheglov, K. V.; Wong, S. S.; Vahalla, K. J.; Flagan, R. C.; Brongersma, M. L.; Polman, A. *Mater. Res. Symp. Soc. Proc*. **1994**, 316.
(17) Heath, J. R.; Shiang, J. J.; Alivisatos, A. P. *J. Chem. Phys*. **1994**, *101*, 1607.
(18) Saunders, W. A.; Sercel, P. C.; Lee, R. B.; Atwater, H. A.; Vahalla, K. J.; Flagan, R. C.; Escorcia-Aparcio, E. J. *Appl. Phys. Lett.* **1993**, *63*, 1549.
(19) Littau, K. A.; Szajowski, P. J.; Muller, A. J.; Kortan, A. R.; Brus, L. E. *J. Phys. Chem*. **1993**, *97*, 1224.
(20) Takagahara, T.; Takeda, K. *Phys. Rev. B* **1992**, *46*, 15578.
(21) Hill, N. A.; Whaley, K. B. *Phys. Rev. Lett.* **1995**, *75*, 1130.
(22) Brus, L. E. *J. Chem. Phys.* **1984**, *80*, 4403.
(23) A number of improvements to this simplified treatment of dielectric screening have been developed (see for example refs 24, 25, and 29) which all give larger Coulomb energies and hence smaller exciton energies.
(24) Wang, L.-W.; Zunger, A. *Phys. Rev. Lett.* **1994**, *73*, 1039.
(25) Hill, N. A.; Whaley, K. B. *Chem. Phys.* **1996**, *210*, 117.
(26) Keating, P. N. *Phys. Rev*. **1966**, *145*, 637.
(27) Pryor, C.; Kim, J.; Wang, L. W.; Williamson, A.; Zunger, A. *J. Appl. Phys.* **1998**, *83*, 2548.
(28) Dietrich, B.; Osten, H. J.; Rücker, H.; Methfessel, M.; Zaumseil, P. *Phys. Rev. B* **1994**, *49*, 17185.
(29) Hill, N. A.; Whaley, K. B. *J. Elec. Mater*. **1996**, *25*, 269.
(30) Vogl, P., et al. *J. Phys. Chem. Solids* **1983**, *44*, 365.
(31) Delerue, C.; Allan, G.; Lannoo, M. *Phys. Rev. B* **1993**, *48*, 11024.
(32) Wang, L. W.; Zunger, A. *J. Phys. Chem*. **1994**, *98*, 2158.
(33) Öğüt, S.; Chelikowsky, J. R.; Louie, S. G. *Phys. Rev. Lett*. **1997**, *79*, 1770.
(34) von Behren, J.; van Buuren, T.; Zacharias, M.; Chimowitz, E. H.; Fauchet, P. M. *Solid State Commun.* **1998**, *105*, 317.
(35) Brey, L.; Tejedor, C.; Vergés, J. A. *Phys. Rev. Lett*. **1987**, *59*, 10022.
(36) Harrison, W. A. *Electronic structure and the properties of solids*; Dover: New York, 1989.
(37) Brey, L.; Tejedor, C. *Phys. Rev. Lett.* **1987**, *59*, 1022.
(38) Harrison, W. A.; Tersoff, J. *J. Vac. Sci. Technol. B* **1986**, *4*, 4.
(39) Van de Walle, C. G.; Martin, R. M. *Phys. Rev. B* **1988**, *34*, 5621.
(40) Tserbak, C., et al. *Phys. Rev. B* **1993**, *47*, 7104.
(41) For simplicity, we have not included surface reconstruction in this calculation. The surface is left in its bulk configuration, with the dangling orbitals pointing to the positions which would be occupied by nearest-neighbor atoms in the bulk material.